The CRISPR Journal
Volume 5, Number 4, 2022

DOI: 10.1089/crispr.2022.0009

The CRISPR Journal

RESEARCH ARTICLE

Enhanced Myogenesis by Silencing Myostatin with Nonviral Delivery of a dCas9 Ribonucleoprotein Complex

Yinwei Chen,[1,2] Lia Banie,[1] Benjamin N. Breyer,[1] Yan Tan,[1] Zhao Wang,[1] Feng Zhou,[1] Guifang Wang,[1] Guiting Lin,[1] Jihong Liu,[3] Lei S. Qi,[4,5] and Tom F. Lue[1,*]

Abstract

Stress urinary incontinence (SUI) and pelvic floor disorder (PFD) are common conditions with limited treatment options in women worldwide. Regenerative therapy to restore urethral striated and pelvic floor muscles represents a valuable therapeutic approach. We aim to determine the CRISPR interference-mediated gene silencing effect of the nonviral delivery of nuclease-deactivated dCas9 ribonucleoprotein (RNP) complex on muscle regeneration at the cellular and molecular level. We designed four myostatin (*MSTN*)-targeting sgRNAs and transfected them into rat myoblast L6 cells together with the dCas9 protein. Myogenesis assay and immunofluorescence staining were performed to evaluate muscle differentiation, while CCK8 assay, cell cycle assay, and 5-ethynyl-2′-deoxyuridine staining were used to measure muscle proliferation. Reverse transcription–polymerase chain reaction and Western blotting were also performed to examine cellular signaling. Myogenic factors (including myosin heavy chain, MSTN, myocardin, and serum response factor) increased significantly after day 5 during myogenesis. MSTN was efficiently silenced after transfecting the dCas9 RNP complex, which significantly promoted more myotube formation and a higher fusion index for L6 cells. In cellular signaling, MSTN repression enhanced the expression of MyoG and MyoD, phosphorylation of Smad2, and the activity of Wnt1/GSK-3β/β-catenin pathway. Moreover, MSTN repression accelerated L6 cell growth with a higher cell proliferation index as well as a higher expression of cyclin D1 and cyclin E. Nonviral delivery of the dCas9 RNP complex significantly promoted myoblast differentiation and proliferation, providing a promising approach to improve muscle regeneration for SUI and PFD. Further characterization and validation of this approach *in vivo* are needed.

Introduction

Stress urinary incontinence (SUI) and pelvic floor disorder (PFD) have profound impacts on the health and wellness of millions of women. The worldwide incidence of SUI was projected to affect 167 million people (a prevalence of 3.3%) by 2018.[1,2] Furthermore, pelvic organ prolapse (POP) has a prevalence of 3–6%, and as high as 50% when evaluated based on vaginal examination.[1,3]

Treatment methods for SUI and PFD include nonsurgical and surgical treatments. Surgical treatments for SUI include various modifications of bladder neck suspension procedures and midurethral slings. For severe (stage 3 and 4) POP, surgical procedures include repair with native tissue, abdominal sacrocolpopexy, and transvaginal mesh. Mesh surgeries for both SUI and POP can be very effective, but many patients experience complications that include infection, mesh erosion, pelvic pain, and dyspareunia. These problems resulted in more than 140,000 lawsuits in the United States alone, and led to a total ban of using mesh for POP in the United States, Australia, and the United Kingdom.[4] Nonsurgical treatment options include pelvic floor exercise, electrical stimulation, biofeedback, topical hormone creams, and bulking agents. Vaginal pessaries, pelvic floor exercise, and biofeedback are used for POP. Although most of these therapies are safe, their efficacy and durability are limited.

Advancing beyond the existing therapies could involve pelvic floor and external urethral sphincter muscle

[1]*Knuppe Molecular Urology Laboratory, Department of Urology, School of Medicine, University of California, San Francisco, San Francisco, California, USA;* [2]*Reproductive Medicine Center, Tongji Hospital, Tongji Medical College, Huazhong University of Science and Technology, Wuhan, China;* [3]*Department of Urology, Tongji Hospital, Tongji Medical College, Huazhong University of Science and Technology, Wuhan, China;* [4]*Department of Bioengineering, Stanford University, Stanford, California, USA; and* [5]*ChEM-H, Stanford University, Stanford, California, USA.*

*Address correspondence to: *Tom F. Lue, Knuppe Molecular Urology Laboratory, Department of Urology, School of Medicine, University of California, San Francisco, 400 Parnassus Avenue, Suite A-630, San Francisco, CA 94143-0738, USA,* E-mail: tom.lue@ucsf.edu

regeneration through different methods. Myostatin (MSTN) is a key negative regulator of skeletal muscle growth, and its absence facilitates muscle regeneration after injury.[5] Currently, the genome editor clustered regularly interspaced short palindromic repeats-Cas9 nuclease-null (CRISPR-Cas9) is effective for targeted modification of MSTN.[6] It has been reported that CRISPR-Cas9-mediated *MSTN* gene knockout promotes striated muscle-derived stem cell differentiation *in vitro*,[7] and the technique has been successfully applied in developing MSTN knockout rabbits, goats, and pigs.[8,9]

In collaboration with Dr. Stanley Qi,[10–12] we have successfully used the CRISPR interference (CRISPRi)-MSTN system to silence *MSTN* and improve myogenesis.[13] In our previous work, we successfully established Zucker fatty rats as a consistent and reliable animal model to study obesity-associated SUI.[14] We used lentivirus to mediate the *MSTN* CRISPRi-dCas9-KRAB gene silencing system *in vitro* in L6 cells and *in vivo* in Zucker rats.[13]

Our previous research adopted a viral system, which is limited in terms of clinical application prospects. In this study, we use a nonviral delivery of the CRISPRi-dCas9-ribonucleoprotein (RNP) complex to inhibit the expression of MSTN and examine the effect on the myogenesis and mechanism involved.

Materials and Methods

Cell culture and transfection

Rat myoblast L6 cells were used in this experiment. The cells were divided into four groups as follows: (I) control; (II) induction; (III) induction+CRISPRi-MSTN-sg; and (IV) mock. In the control and induction groups, cells were cultured in Dulbecco's modified Eagle's medium (DMEM) containing 10% fetal bovine serum (FBS) and 2% horse serum (HS), respectively. In the induction+CRISPRi-MSTN-sg group, 2×10^5 L6 cells were seeded in each six-well plate and cultured in DMEM containing 10% FBS. The following day, the medium was treated with 50 μL of CRISPRi-dCas9-RNP complex (four guide RNAs: *MSTN*-sg1, *MSTN*-sg2, *MSTN*-sg3, and *MSTN*-sg4). In the mock group, the cells were treated with dCas9 RNPs (Integrated DNA Technologies, Inc., Coralville, IA) only without single-guide RNA (sgRNA). One day after transduction, the medium was replaced by fresh DMEM with 2% HS, and 5 days after transduction, cells were harvested for myotube formation assay and gene expression assay.

Nonviral delivery of CRISPRi/dCas9-RNP complex (reverse transfection)

The MSTN sgRNAs were designed by using https://portals.broadinstitute.org/gpp/public/analysis-tools/sgrna-design-crisprai and https://www.ncbi.nlm.nih.gov/gene/29152 The 2′-*O*-methyl 3′ phosphorothioate modification in the first and last three nucleotides were applied to all four sgRNAs. The sequences of sgRNA are as follows: (1) MSTN-sg1 (TGGCCCAGTGGATCTAAATG) UGGCCCAGUGGAUCUAAAUG; (2) MSTN-sg2 (TGTCCTCATTTAGATCCACT) UGUCCUCAUUUAGAUCCACU; (3) MSTN-sg3 (CAGCAGCAATCAGCACAAAC) CAGCAGCAAUCAGCACAAAC; and (4) MSTN-sg4 (GCTGATTGCTGCTGGCCCAG) GCUGAUUGCUGCUGGCCCAG. The sgRNAs were ordered from Synthego (Menlo Park, CA).

The L6 cells were seeded and incubated in a 37°C/5% CO_2 incubator overnight so that they are ~70% confluent on the day of transfection. The 24-well cell culture plates were prewarmed with 500 μL of normal growth medium in each well. The same volume of RNP solution+cells (225 μL) was added to each well of each plate. The L6 cells on the first plate were lysed and processed to analyze editing efficiency. The cells on other plates were cultured for use in assays, banking, and/or single-cell cloning.

The sgRNA and dCas9 protein V3 (Integrated DNA Technologies, Inc.) were diluted to 3 μM working stock concentrations. The RNP complexes of sgRNA to dCas9 were assembled in a ratio of 1.3:1, and a total of 28.3 μL of RNPs was added in a microcentrifuge tube.

The Lipofectamine™ CRISPRMAX™ Reagent (1.5 μL) was mixed with Opti-MEM™ I Reduced Serum Medium (25 μL) in another tube to form transfection solution. Both tubes were incubated for 5 min at room temperature (RT) and then the RNP complexes and transfection solution were mixed and incubated for 5–10 min at RT.

The L6 cells were resuspended in the growth medium after trypsin digestion. For each reaction, the RNP-transfection solution (50 μL) was mixed with the cells (500 μL) in a microcentrifuge tube to a total volume of 550 μL and seeded into 2×24-well plates by adding 225–250 μL per replicate well. The cells were cultured in a humidified 37°C/5% CO_2 incubator for 2–3 days and then treated with the above procedures.

To further confirm this effect, C2C12 cells and primary rat urethral muscle-derived stem cells were also used for the myotube formation assay.

Myogenesis assay and immunofluorescence staining

With stimulation from trigger factors, myoblast cells differentiate into myocytes and then the myotube forms from the fusion of myocytes. This biological process is termed as myogenesis. We used immunofluorescence (IF) staining to check for myotube formation in the L6

cells after treatment. The cells were fixed with ice-cold methanol for 8 min, permeabilized with 0.05% Triton X-100 for 5 min, and blocked with 5% normal HS in phosphate-buffered saline (PBS) for 1 h at RT. Next, they were incubated with the goat anti-myosin heavy chain (MHC) antibody for 1 h at RT. After washing with PBS three times, the cells were incubated with the DexRed-conjugated goat anti-rabbit antibody for 1 h at RT. After three washes with PBS, the cells were stained with 4′,6-diamidino-2-phenylindole (DAPI; for nuclear staining) for 5 min. Finally, the IF slides were examined under a fluorescence microscope and photographed.

Cell proliferation assay with CCK8 assay and 5-ethynyl-2′-deoxyuridine incorporation

The effect of MSTN inhibition with CRISPRi-dCas9-RNP system on L6 cell proliferation was assayed with the CellTiter-96 kit (Promega, Inc., Madison, WI). All the reagents were dissolved in PBS at 1000 mg/mL as stock solution. Further dilutions were made in serum-free DMEM supplemented with 0.1% bovine serum albumin (BSA) and were assayed in a flat-bottom 96-well cell culture plate. L6 cells at 80% confluence were rinsed twice with PBS, trypsinized, and resuspended in serum-free DMEM (supplemented with 0.1% BSA) at 10^5 cells/mL. Aliquots of 50 μL of the cell suspension were then transferred to the 96-well plate so that each well contained 5000 cells in a final volume of 100 μL.

In general, 20 μL of CCK8 solution reagent (MedChemExpress, NJ) was added to each well. After 2 h of further incubation at 37°C in the humidified 5% CO_2 incubator, color development, which reflects the cell number, was recorded with a plate reader (Molecular Devices Corp., Sunnyvale, CA) at 490-nm absorbency. For the EdU incorporation assay, 10 μM of EdU was added to cells overnight, and EdU was checked with Click-iT reaction cocktail conjugated with Alexa594-azide (EdU Click-iT Cat# C10339; Invitrogen, La Jolla, CA) for 30 min at RT. After nuclear staining with DAPI for 5 min, the cells were examined under a fluorescence microscope and photographed. The cell cycle assay was performed with propidium iodide staining and flow cytometry as previously reported.[15] All assays were duplicated in each experiment, and all data presented as the mean of three independent experiments.

Reverse transcription–polymerase chain reaction

As previously reported,[16–18] total RNA was extracted using the High Pure RNA Isolation Kit (Roche, Germany) following the kit instructions. Total RNA (2.5 μg) was annealed to 0.4 μg of oligo-dT primer in a volume of 12 μL. Then, 4 μL of 5×buffer, 2 μL of 0.1 M dithiothreitol, 1 μL of 10 mM dNTP, and 1 μL of SuperScript reverse transcriptase (Invitrogen) were added to bring the final volume to 20 μL. After 1 h of incubation at 42°C, the mixture was incubated at 70°C for 10 min to inactivate the reverse transcriptase. Then, 80 μL of Tris-EDTA buffer was added to make a 5×diluted complementary DNA library, from which 1 μL was used for reverse transcription–polymerase chain reaction (PCR).

The cycling program was set for 35 cycles of 94°C for 10 s, 55°C for 10 s, and 72°C for 10 s, followed by one cycle of 72°C for 5 min. The PCR products were electrophoresed in 1.5% agarose gels, visualized by ultraviolet fluorescence, and recorded by a digital camera. Data were analyzed by ChemiImager-4000 software (version 4.04; Alpha Innotech Corporation, San Leandro, CA). Primer sequences are presented in Table 1.

Western blot for cellular signaling assay

The cellular protein samples were prepared by homogenization of cells in a lysis buffer containing 1% IGEPAL CA-630, 0.5% sodium deoxycholate, 0.1% sodium dodecyl sulfate, aprotinin (10 mg/mL), leupeptin (10 mg/mL), and PBS. Cell lysates containing 20 μg of protein were electrophoresed in sodium dodecyl sulfate–polyacrylamide gel electrophoresis and then transferred to a polyvinylidene fluoride membrane (Millipore Corp, Bedford, MA). The membrane was stained with Ponceau S to verify the integrity of the transferred proteins and to monitor the unbiased transfer of all protein samples. Detection of target proteins on the membranes was performed with an electrochemiluminescence kit (Amersham Life Sciences, Inc., Arlington Heights, IL) with the use of primary antibodies for MHC, MSTN, MyoG, MyoD, p-Smad2 and Smad2, Wnt1, GSK-3β, β-catenin, and β-actin (antibody information is presented in Table 2).

Table 1. Primer sequence used for reverse transcription–polymerase chain reaction

Genes	*Primer sequence (5′→ 3′)*
MHC-F	GACTACAACATCGCTGGCTG
MHC-R	CCCTGAAGAGAGCTGACACA
MSTN-F	GCTCTTTGGAAGATGACGA
MSTN-R	CTTGCATTAGAAAGTCAGACTC
MyoCD-F	GTGCCAAGACTGAAGACTC
MyoCD-R	GGAGAATGTGCATATTAACCAG
SRF-F	CATGAAGAAGGCTTATGAGCTG
SRF-R	TACACATGGCCTGTCTCAC
α-SMA-F	CATCATGCGTCTGGACTTGG
α-SMA-R	CCAGGGAAGAAGAGGAAGCA
β-Actin-F	AAAGAAAGGGTGTAAAACGCA
β-Actin-R	TCAGGTCATCACTATCGGCAAT

MHC, myosin heavy chain; MSTN, myostatin; MyoCD, myocardin; SMA, smooth muscle actin; SRF, serum response factor.

Table 2. Antibodies used for Western blot

Antibody	*Dilution (Supplier)*
Anti-MHC	1:1000 (Abcam, Cambridge, MA)
Anti-MSTN	1:1000 (Santa Cruz Biotech, Santa Cruz, CA)
Anti-MyoG	1:1000 (Santa Cruz Biotech)
Anti-MyoD	1:1000 (Santa Cruz Biotech)
Anti-p-Smad2	1:1000 (Santa Cruz Biotech)
Anti-Smad2	1:1000 (Santa Cruz Biotech)
Anti-Wnt1	1:1000 (Santa Cruz Biotech)
Anti-GSK-3β	1:1000 (Santa Cruz Biotech)
Anti-β-catenin	1:1000 (Santa Cruz Biotech)
Anti-β-actin	1:1000 (Invitrogen, Carlsbad, CA)
HRP-linked goat anti-mouse	1:10,000 (Invitrogen)
HRP-linked goat anti-rabbit	1:10,000 (Invitrogen)

HRP, horseradish peroxidase.

After hybridization of secondary antibodies, the resulting images were analyzed with the ChemiImager 4000 (Alpha Innotech) to determine the integrated density value of each protein band.

Statistical analyses

Results were analyzed using GraphPad Prism version 5.0 (GraphPad Software, San Diego, CA) and expressed as mean ± standard error. Statistical analyses were performed using one-way analysis of variance followed by the Tukey's *post hoc* test for multiple comparisons. Differences among groups were considered significant at $p < 0.05$.

Results

Time alteration of myogenic factors

To clarify the timing of myogenic factor alteration for L6 cells, we chose four time points and collected both RNA and protein samples. As shown in Figure 1a and b, *MHC, MSTN, myocardin (MyoCD)*, and serum response factor (*SRF*) were at low levels in both the control and induction groups in the first 3 days, and they gradually increased on days 4 and 5. RNA levels of aforementioned factors were significantly higher in the induction group than in the control group. However, the RNA level of α-smooth muscle actin remained stable during the induction period of 6 days. Western blot (WB) results confirmed this finding.

On an upward trend, protein levels of MHC and MSTN evidently increased more in the induction group than in the control group (Fig. 1c, d). This finding suggests that MHC, MSTN, MyoCD, and SRF are valuable factors

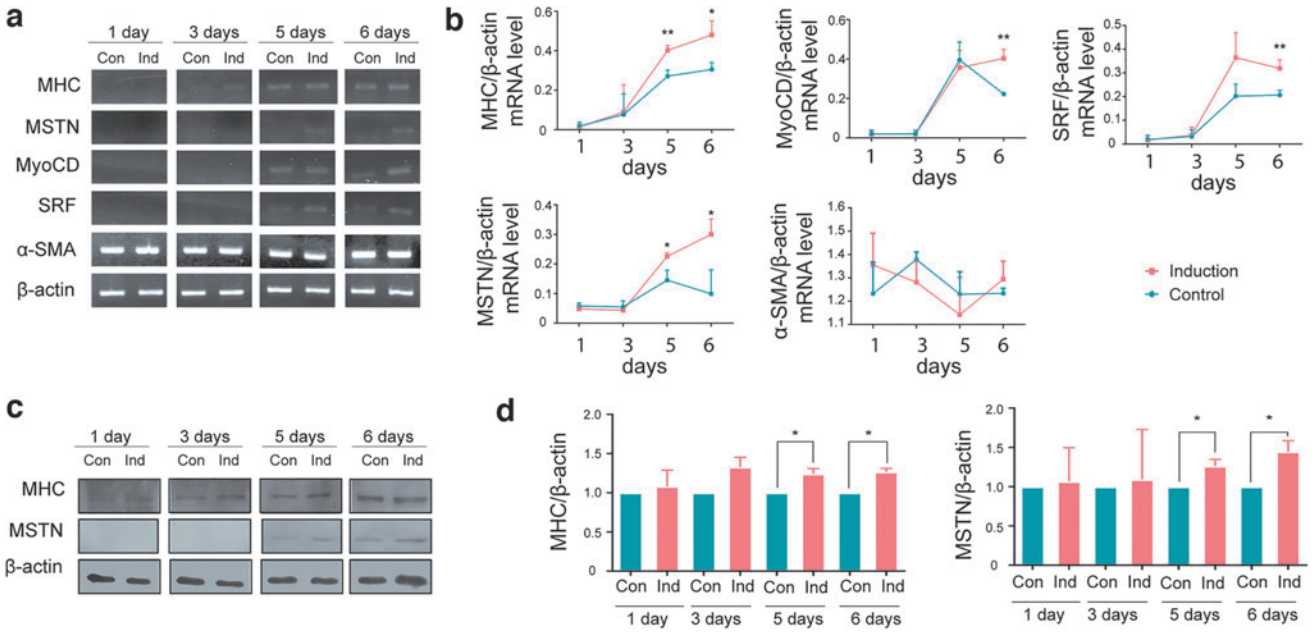

FIG. 1. Changes of myogenic factors during L6 cell differentiation. **(a)** PCR results for *MHC, MSTN, MyoCD, SRF, α-SMA*, and *β-actin* at different time points (1, 3, 5, 6 days) in the control and induction groups. **(b)** mRNA levels of *MHC, MSTN, MyoCD, SRF,* and *α-SMA* compared with that of β-actin in the two groups. **(c)** WB results for MHC, MSTN, and β-actin at different time points (1, 3, 5, 6 days) in the control and induction groups. **(d)** Relative expression level of *MHC* and *MSTN* compared with that of *β-actin* in the two groups. Data are presented as mean ± SD from three independent replicates. *$p < 0.05$, **$p < 0.01$, and ***$p < 0.001$. Con, control; Ind. induction; MHC, myosin heavy chain; MSTN, myostatin; MyoCD, myocardin; PCR, polymerase chain reaction; SD, standard deviation; SMA, smooth muscle actin; SRF, serum response factor; WB, Western blot.

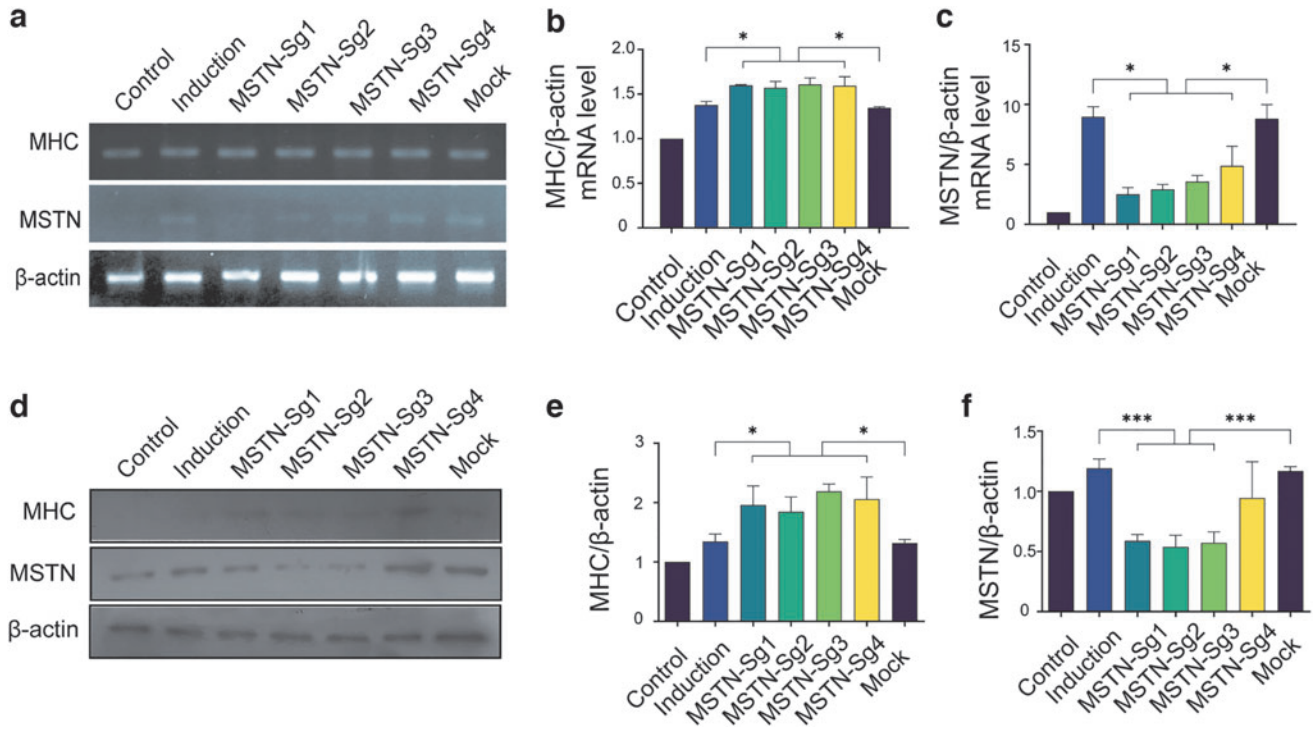

FIG. 2. MSTN-RNP complexes successfully silenced *MSTN* expression. **(a)** PCR results for MHC and MSTN in the seven groups. Relative mRNA levels of *MHC* **(b)** and *MSTN* **(c)** compared with that of *β-actin* in the seven groups. **(d)** WB results for MHC and MSTN in the seven groups. Relative density of MHC **(e)** and MSTN **(f)** compared with that of β-actin in the seven groups. $*p < 0.05$ and $***p < 0.001$. RNP, ribonucleoprotein.

during L6 cell differentiation. Days 5 and 6 are the suitable timing to determine the changes of myogenic factors in the following experiments.

Myotube formation after MSTN silence

In this study, we used the nonviral delivery of CRISPRi-dCas9-RNP complex to silence the MSTN expression and screened four MSTN-sgRNA sequences to evaluate the effect. In both the RNA and protein levels, MSTN expression noticeably increased in the induction group compared with the control group (Fig. 2a, c, d, f). MSTN was remarkably reduced in the MSTN-Sg1, Sg2, and Sg3 groups compared with the induction and mock groups. Especially for the MSTN-Sg2 and Sg3 groups, *MSTN* mRNA levels were reduced by about 60–70%, while protein levels were reduced by about 50–60%.

On the contrary, MHC expression was remarkably higher in the four MSTN-Sg groups relative to the induction and mock groups (Fig. 2a, b, d, e), and the MSTN-Sg3 group had the highest expression of MHC. Similarly, IF results also showed that these four MSTN-Sg groups had the significantly larger positive area of MHC (Fig. 3a, b). We found that these four groups had more myotube numbers and higher fusion indexes of myotube compared with the other groups (Fig. 3c, d), with the MSTN-Sg3 showing the best indicators. Our results suggest that the RNP system successfully transferred dCas9 protein and sgRNA into the L6 cells and further reduced MSTN expression. The myotube formation from C2C12 and primary rat urethral muscle-derived stem cells after MSTN silence also confirmed similar results (Supplementary Figs. S1 and S2).

The nuclear movement is required in the myoblast fusion and myofiber generation.[19] We found that although these nuclei tend to be spread, and they still converge in the center of the myotube in the induction control and mock groups. However, the nuclei have been apparently uniformly speared in that long axis of the myotube in the MSTN 1–2 groups. With the enlargement of myotubes, more nuclei began to migrate to the periphery in the MSTN 3–4 groups, and their position has been significantly away from the center of the long axis. The results indicate that MSTN can promote nuclear aggregation and rearrangement, and the MSTN-Sg3 had a strong effect (Supplementary Fig. S3).

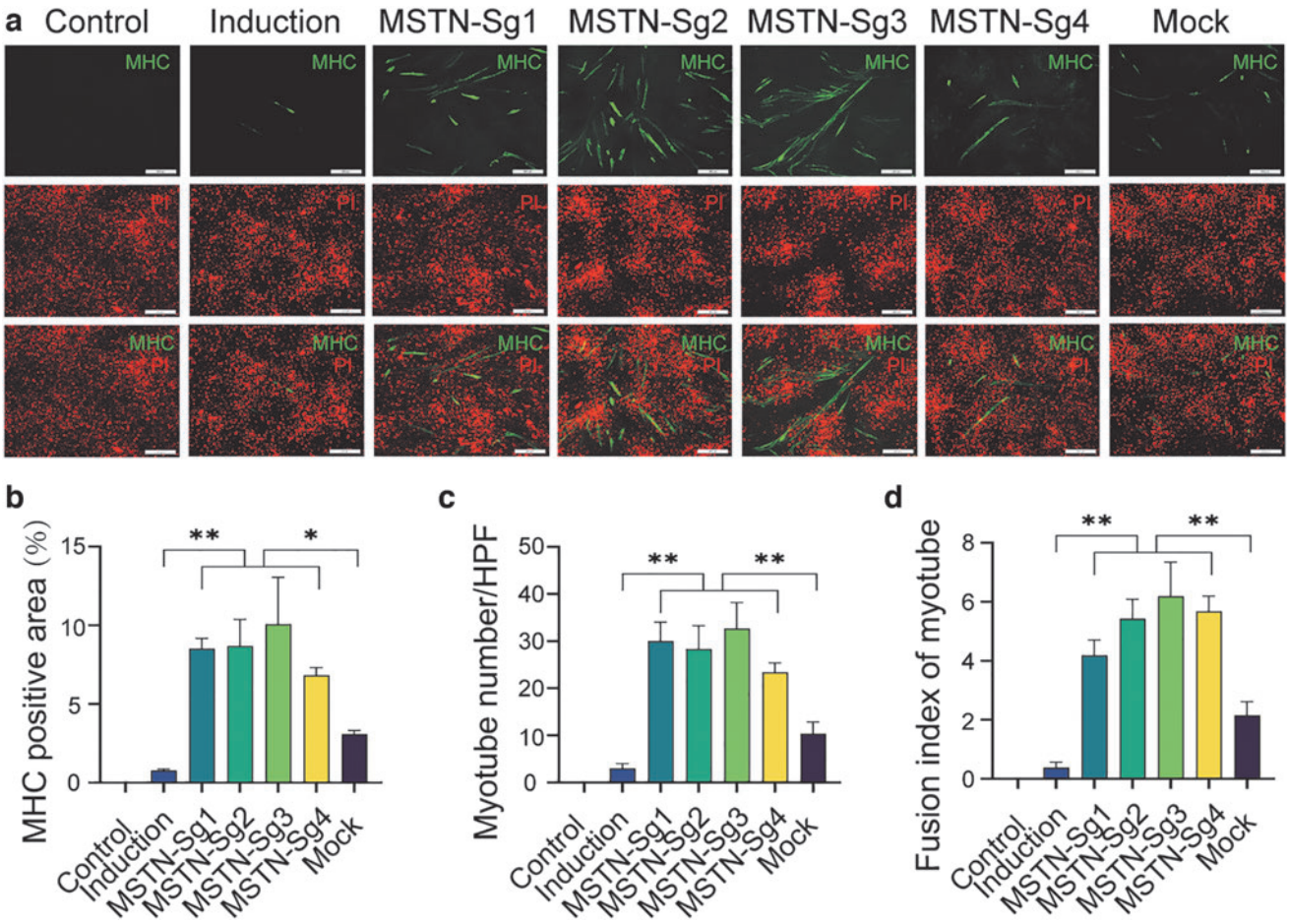

FIG. 3. MSTN silence promoted myotube formation. **(a)** Immunofluorescence results for MHC (green) and nucleus (red) in L6 cells of the seven groups (control, induction, MSTN-Sg1, MSTN-Sg2, MSTN-Sg3, MSTN-Sg4, and mock) after transfection (magnification 100×), scale bars = 200 μm. Semiquantitative analysis of MHC-positive area **(b)**, myotube number/HPF **(c)**, and fusion index **(d)** in the seven groups. Fusion index (%) = (number of nuclei in myotubes)/(total number of nuclei) × 100%. Data are presented as mean ± SD from three independent replicates. *$p < 0.05$ and **$p < 0.01$.

Change of signaling pathway activity after MSTN silence

Given that the sgRNA-3 achieved the lowest MSTN level and highest MHC level, we chose sgRNA-3 to perform the following experiments. First, we measured the myogenic factor of MyoG and MyoD. WB results showed that MSTN silence enhanced the expression of MyoG and MyoD compared with the induction and mock groups (Fig. 4a, c, d). The phosphorylation of Smad2 is the classical downstream signaling cascade after MSTN binds to its activin type II receptor.[20] We found that total Smad2 and the ratio of p-Smad2 to Smad2 increased in the induction group compared with the control group. MSTN silence noticeably inhibited Smad2 expression and its phosphorylation level (Fig. 4a, e, f). It has also been reported that MSTN activation largely affects the activity of Wnt/β-catenin signaling.[21]

We found that Wnt1 and β-catenin were significantly inhibited in the induction group, while MSTN silence significantly promoted Wnt1 and β-catenin expression, while GSK-3β showed the opposite trend (Fig. 4g–j). Data suggest that myotube formation induced by the MSTN-CRISPRi-dCas9 RNP complex was associated with phosphorylation of the Smad2 and Wnt1/GSK-3β/β-catenin pathway.

Cell proliferation after MSTN silence

To evaluate whether MSTN silence influenced the proliferation of L6 cells, we performed EdU staining and CCK8 assay. As shown in Figure 5a and b, the percentage of EdU-positive cells was lowest in the induction group, whereas MSTN silence greatly elevated the percentage. Similarly, results of CCK8 assay showed that although

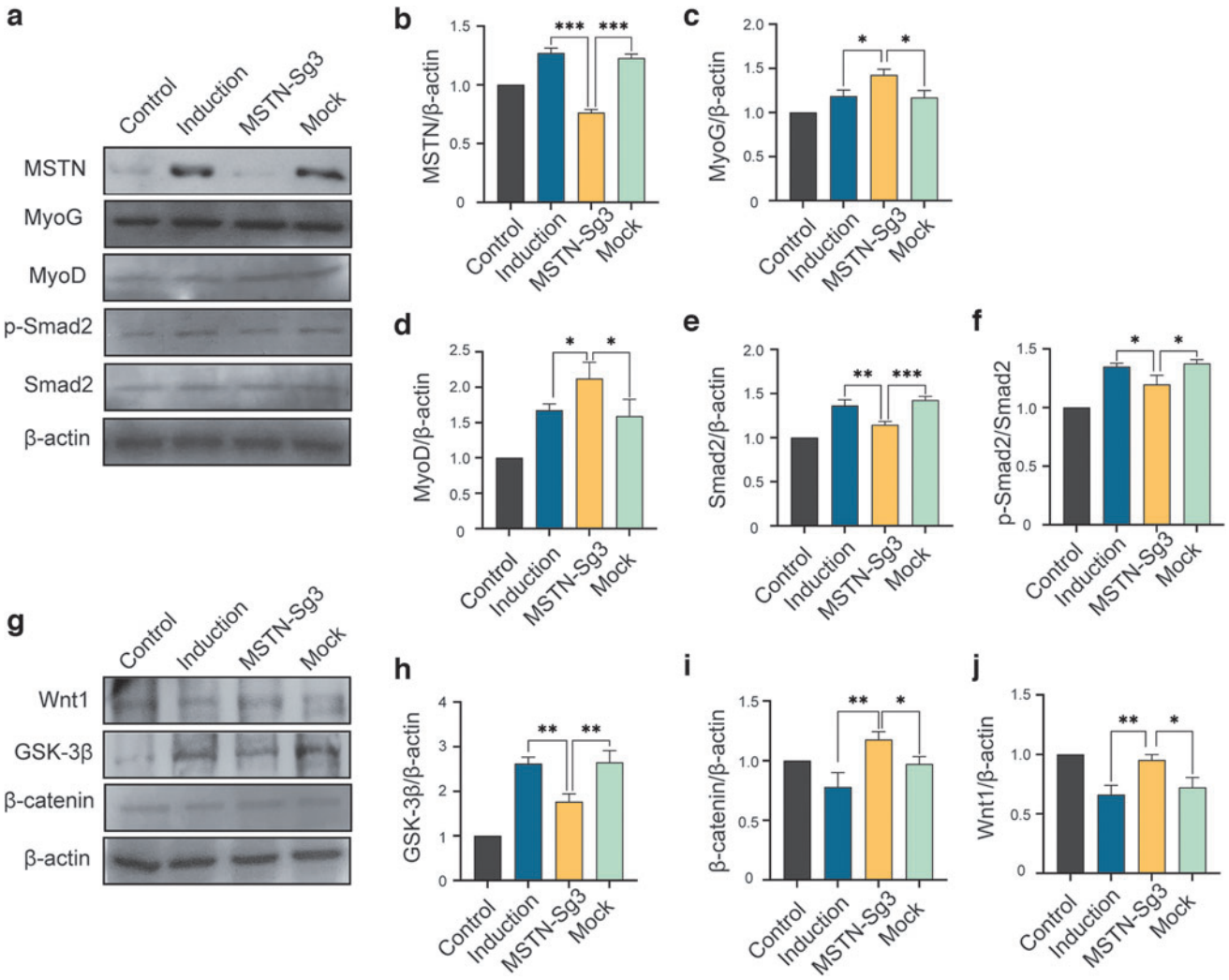

FIG. 4. MSTN silence altered p-Smad2/Smad2 and Wnt1/GSK-3β/β-catenin pathways. **(a)** WB results for MSTN, MyoG, MyoD, p-Smad2, and Smad2 in the four groups (control, induction, MSTN-Sg3, and mock) after transfection. Relative density of MSTN **(b)**, MyoG **(c)**, MyoD **(d)**, p-Smad2 **(e)**, and Smad2 **(f)** compared with that of β-actin in the four groups. **(g)** WB results for Wnt1, GSK-3β, and β-catenin in the four groups. Relative density of Wnt1 **(h)**, GSK-3β **(i)**, and β-catenin **(j)** compared with that of β-actin in the four groups. Data are presented as mean ± SD from three independent replicates. *$p < 0.05$, **$p < 0.01$, and ***$p < 0.001$. GSK-3β, glycogen synthase kinase 3 beta; MyoD, myogenic differentiation 1; MyoG, myogenin; Wnt1, Wnt family member 1.

the numbers of L6 cell were all increasing among the four groups, there was a significant difference between the MSTN-Sg3 and induction groups (Fig. 5c). There was a significantly higher cell proliferation index in the MSTN-Sg3 group compared with the induction group, which means that more L6 cells entered the S+G2/M phase (Fig. 6a, b). WB results further validated that MSTN silence remarkably enhanced cyclin D1 and cyclin E expression relative to the induction group (Fig. 6c–e). This finding suggests that MSTN silence promotes cell cycle and proliferation for L6 cells.

Discussion

The CRISPR-Cas9 system, a revolutionary genetic editing tool, has shown a great potential in medical treatment and biological research. It has two important components: Cas9 nuclease and single-guide RNA (sgRNA). sgRNA directs the constructs to the DNA target site, and stimulates Cas9 to cleave the DNA strands. DNA double-strand break repair is mainly associated with two conserved mechanisms: nonhomologous end-joining and homology-directed repair (HDR) pathway.[20] With a template DNA, the HDR pathway helps researchers to induce the precise

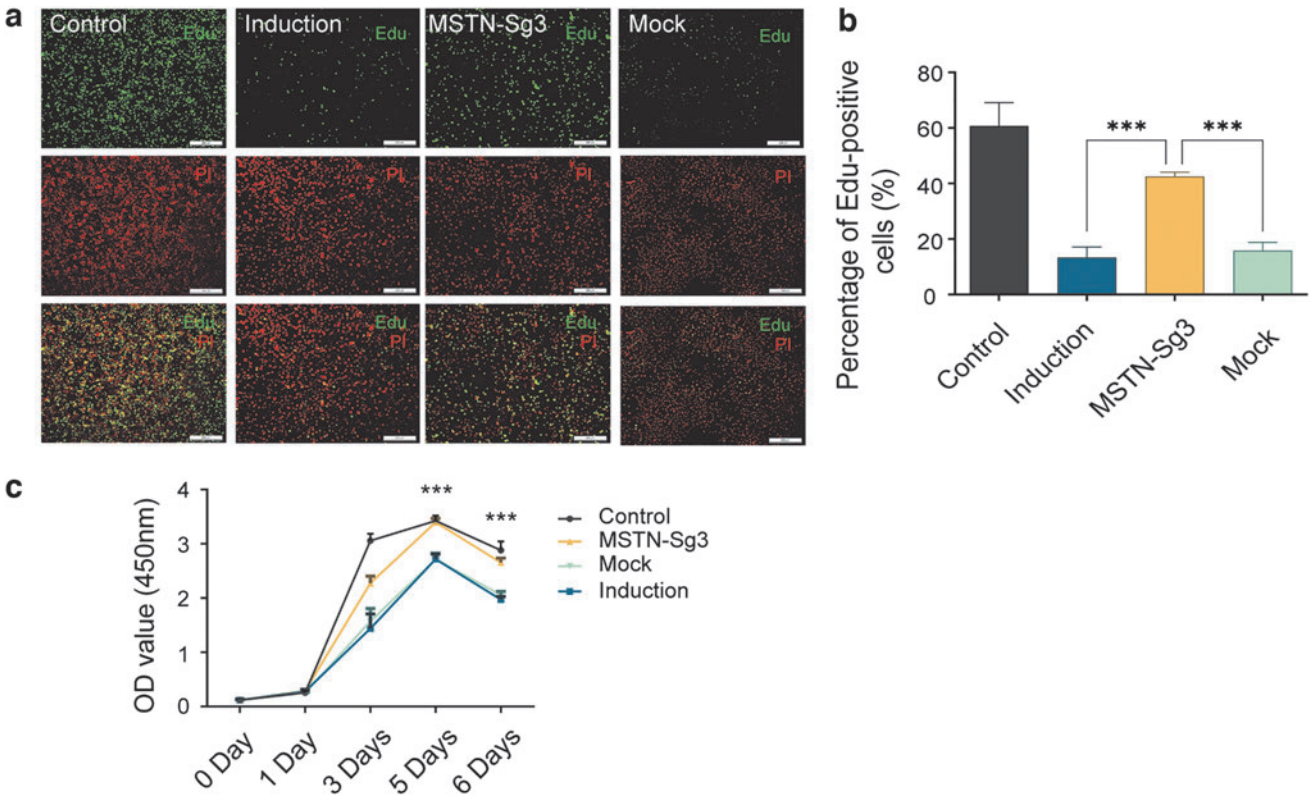

FIG. 5. MSTN silencing promoted L6 cell proliferation. **(a)** EdU staining result for L6 cells in the four groups (control, induction, MSTN-Sg3, and mock) after transfection (magnification 100×), scale bars = 200 μm. **(b)** The percentage of the EdU-positive cells in the four groups. **(c)** The proliferation of L6 cells in the four groups was determined by the CCK8 assay. ***$p < 0.001$. EdU, 5-ethynyl-2′-deoxyuridine.

knockin and knockout sequence in the target site for gene modification.[21–23] As for catalytically dead Cas9, it has been widely used for gene silencing in eukaryotic cells through CRISPRi due to its absence of endonuclease activity.[24] Efficient delivery is vital and acts as the precondition for the function of CRISPR/dCas9 system.

Compared with plasmid DNA and messenger RNA, delivery of RNP complex has the distinct advantage, such as high editing efficiency, less off-target effects, and lower immunogenicity.[24,25] There are three ways to deliver the RNP components into cells and organs, including viral, nonviral, and physical methods. Generally, the nonviral method is preferred because it does not have virus-related side effects such as carcinogenesis, restricted encapsulating capacity, and immunogenicity.[25]

In 2012, Dever *et al.* reported that using the RNP complex could successfully obtain homologous-recombination-mediated modification at the HBB locus in $CD34^+$ hematopoietic stem cells to cure the β-hemoglobinopathies.[26] RNP complex not only showed broad application prospects in the field of stem cells (human pluripotent stem cells and induced pluripotent stem cells),[26–28] but also exhibited good effects in *in vivo* studies. In the field of muscle dysfunction, Cas9 RNP has been utilized to delete the mutated exon 23, which is the cause of Duchenne muscular dystrophy in a mouse model. This resulted in the genetic deletion as well as improved muscle function.[29]

However, there are few reports on the use of RNP complex in the treatment of urinary incontinence. In this study, we first used the cationic lipid-based vectors to transfer the RNP components into L6 cells to silence the *MSTN* gene. We found that the MSTN-Sg3 RNP complex significantly reduced MSTN expression, and the mRNA levels decreased about 60–70%. It suggests that nonviral delivery of CRISPRi-dCas9-RNP complex into L6 cells is feasible, which lays a good foundation for further enhancing muscle regeneration *in vivo*.

During the myotube formation, low concentration of serum stimulates the significant increase of key myogenic factors at day 5, including MHC, MSTN, and MyoCD (Fig. 1). Usually, most studies on the differentiation of myoblasts have selected the induction time of days 5–7,[30,31] and this allows time for differential myogenic factors to take effect. In this study, we focused on the

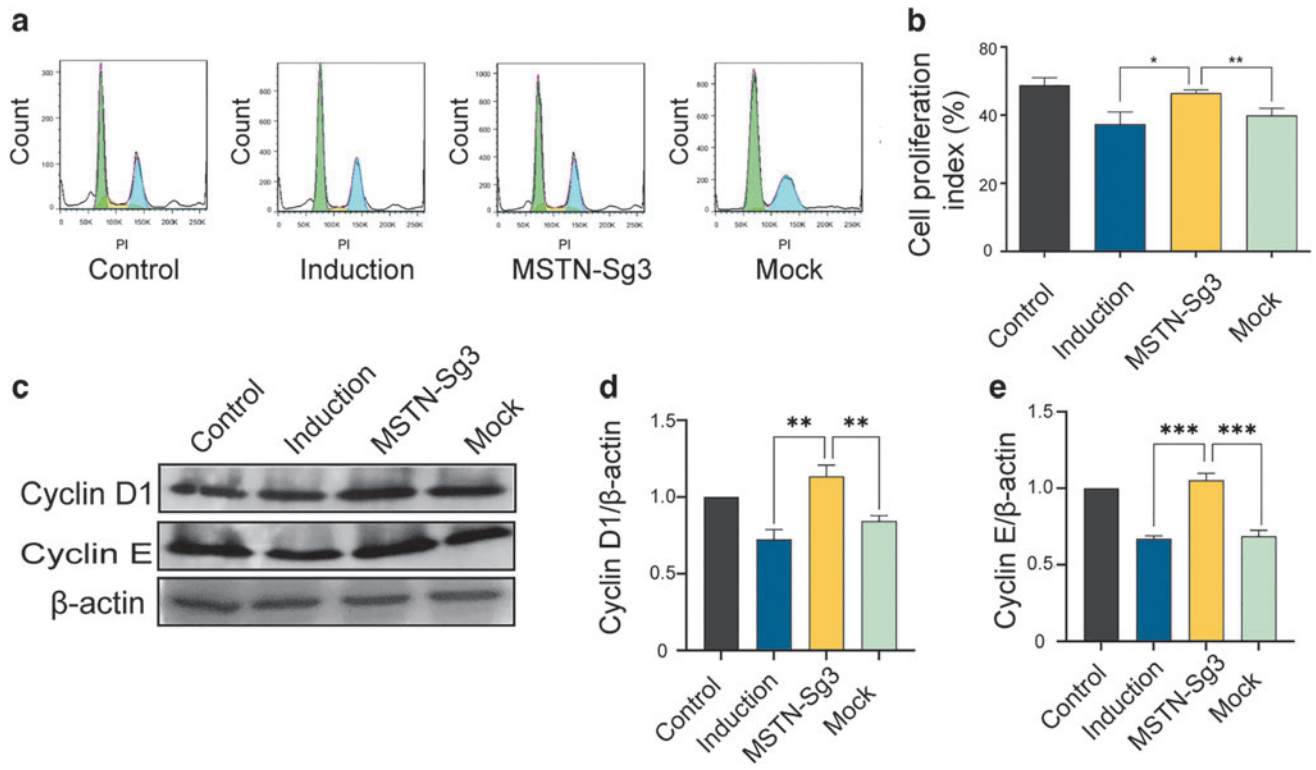

FIG. 6. MSTN silencing altered cell cycle. **(a)** Distribution of cell cycle for L6 cells in the four groups. **(b)** The cell proliferation rate in the four groups. **(c)** WB results for cyclin D1 and cyclin E in the four groups. Relative density of cyclin D1 **(d)** and cyclin E **(e)** compared with that of β-actin in the four groups. Cell proliferation index (%) = (number of cell in S+G2/M phase)/(number of cell in G0/G1+S+G2/M phase) × 100%. Data are presented as mean ± SD from three independent replicates. *$p < 0.05$, **$p < 0.01$, and ***$p < 0.001$.

potential of MSTN to improve muscle regeneration. MSTN has been reported to be a negative modulator of myogenesis, and it has a robust effect on growth and differentiation of myoblasts, proliferation of satellite cells, and thickening of muscle fibers.[32–34]

In this study, silencing MSTN using RNP complex could lead to more myotube formation and a higher fusion index in L6 cells. MSTN is capable of triggering the phosphorylation of Smad2 and inhibiting Akt in the cytoplasm. Smad2/3/4 complex further translocates into the nucleus to affect the transcription of genes involved in muscle atrophy.[35,36] Data consistently showed that Smad2 phosphorylation was remarkably lower in the MSTN RNP-treated group than that in the induction group, while expression of MyoG and MyoD was remarkably higher than that of induction groups. Growing evidence has shown a signal interaction between the MSTN and Wnt/β-catenin pathway.[37,38] Our study confirmed that inhibiting MSTN can reduce the activity of Wnt1/GSK-3β/β-catenin pathway in L6 cells. However, the intermediate factor between the MSTN and Wnt signaling needs to be investigated further.

During muscle regeneration, critical biological processes include satellite cell proliferation to replenish the muscle stem cell pool and satellite cell differentiation to repair muscle damage. Significant evidence shows that MSTN is negatively associated with muscle cell proliferation validated by genome mutagenesis,[39] miRNA inference,[40] and artificial overexpression.[41] It was reported that the mammalian target of rapamycin (mTOR) and AKT/FoxO1 pathways participated in MSTN inhibition-induced proliferation in cultured Japanese flounder muscle cells.[41] Huang *et al.* revealed that MSTN-mediated c-Jun N-terminal kinase signaling pathway was activated in both proliferating and differentiating mouse myoblasts.[42] Furthermore, autophagy and ubiquitin–proteasome act as critical approaches for MSTN-mediated muscle catabolism in chronic kidney disease.[43] Consistently, we found that silencing MSTN using the RNP complex enhanced L6 cell proliferation together with the higher level of EdU uptake and higher proliferation index. The elevated cyclin D1 and E were required in this process.

It is well established that Wnt signaling plays an important role in regulating cell proliferation, and Cyclin

D1 acts as the target gene of the Wnt/β–catenin pathway.[44] Therefore, it is reasonable to assume that silencing MSTN-induced proliferation is closely related to the Wnt signaling-mediated cyclin increase.

There are several limitations of our study. First, this is a cellular and molecular experiment, and the efficacy and durability of RNP treatment require validation in animal model and multiple cell lines, especially for human primary myoblasts. Second, although the four MSTN sgRNAs were all efficient, more potent sgRNAs should be explored. In addition, our previous work demonstrated that microenergy acoustic pulse (MAP) treatment activates urethral striated muscle regeneration.[12] It would be valuable to combine both MAP and nonviral delivery of MSTN RNP complex to see their synergistic potential.

Conclusion

Downregulation of MSTN with nonviral delivery of CRISPRi-dCas9-RNP complex significantly enhanced myogenesis, which may be a potential clinical therapeutic approach.

Authors' Contributions

Conceptualization, G.L., L.S.Q., and T.F.L. Methodology, Y.C., L.B., Y.T., Z.W., F.Z., G.W., J.L., and G.L. Investigation, Y.C., L.B., Y.T., Z.W., F.Z., G.W., and G.L. Writing—original draft, Y.C. and G.L. Writing—review and editing, B.N.B., G.L., L.S.Q., and T.F.L. Funding acquisition, G.L. and T.F.L. Resources, G.L and L.B. Supervision, L.S.Q., G.L., and T.F.L.

All the coauthors have reviewed and approved of the article before submission. This article has been submitted solely to this journal and is not published, in press, or submitted elsewhere. It is not under consideration by another journal or other publications and has not been previously published.

Acknowledgments

Research reported in this publication was supported by the National Institute of Diabetes and Digestive and Kidney Diseases of the National Institutes of Health under award number 1R01DK124609. L.S.Q. acknowledges support from the Stanford Maternal and Child Health Research Institute (MCHRI) through the Uytengsu-Hamilton 22q11 Neuropsychiatry Research Award Program. The content is solely the responsibility of the authors and does not necessarily represent the official views of the National Institutes of Health.

Author Disclosure Statement

No competing financial interests exist.

Funding Information

This article was funded by the NIDDK of the National Institutes of Health under award number 1R01DK124609.

Supplementary Material

Supplementary Figure S1
Supplementary Figure S2
Supplementary Figure S3

References

1. D'Angelo W, Dziki J, Badylak SF. The challenge of stress incontinence and pelvic organ prolapse: Revisiting biologic mesh materials. *Curr Opin Urol.* 2019;29:437–442. DOI: 10.1097/MOU.0000000000000645.
2. Irwin DE, Kopp ZS, Agatep B, et al. Worldwide prevalence estimates of lower urinary tract symptoms, overactive bladder, urinary incontinence and bladder outlet obstruction. *BJU Int.* 2011;108:1132–1138. DOI: 10.1111/j.1464-410X.2010.09993.x.
3. Barber MD, Maher C. Apical prolapse. *Int Urogynecol J.* 2013;24:1815–1833. DOI: 10.1007/s00192-013-2172-1.
4. FDA. Urogynecologic Surgical Mesh Implants. https://www.fda.gov/medical-devices/implants-and-prosthetics/urogynecologic-surgical-mesh-implants [Last accessed: October 16, 2021].
5. Kirk S, Oldham J, Kambadur R, et al. Myostatin regulation during skeletal muscle regeneration. *J Cell Physiol.* 2000;184:356–363. DOI: 10.1002/1097-4652(200009)184:3 <356::AID-JCP10>3.0.CO;2-R.
6. Zhang J, Liu J, Yang W, et al. Comparison of gene editing efficiencies of CRISPR/Cas9 and TALEN for generation of MSTN knock-out cashmere goats. *Theriogenology.* 2019;132:1–11. DOI: 10.1016/j.theriogenology.2019.03.029.
7. Zhang Y, Wang Y, Yulin B, et al. CRISPR/Cas9-mediated sheep MSTN gene knockout and promote sSMSCs differentiation. *J Cell Biochem.* 2018. [Epub ahead of print]; DOI: 10.1002/jcb.27474.
8. Wang K, Tang X, Xie Z, et al. CRISPR/Cas9-mediated knockout of myostatin in Chinese indigenous Erhualian pigs. *Transgenic Res.* 2017;26:799–805. DOI: 10.1007/s11248-017-0044-z.
9. Guo R, Wan Y, Xu D, et al. Generation and evaluation of Myostatin knockout rabbits and goats using CRISPR/Cas9 system. *Sci Rep.* 2016;6:29855. DOI: 10.1038/srep29855.
10. Larson MH, Gilbert LA, Wang X, et al. CRISPR interference (CRISPRi) for sequence-specific control of gene expression. *Nat Protoc.* 2013;8:2180–2196. DOI: 10.1038/nprot.2013.132.
11. Qi LS, Larson MH, Gilbert LA, et al. Repurposing CRISPR as an RNA-guided platform for sequence-specific control of gene expression. *Cell.* 2013;152:1173–1183. DOI: 10.1016/j.cell.2013.02.022.
12. Wang B, Zhou J, Banie L, et al. Low-intensity extracorporeal shock wave therapy promotes myogenesis through PERK/ATF4 pathway. *Neurourol Urodyn.* 2018;37:699–707. DOI: 10.1002/nau.23380.
13. Yuan H, Ruan Y, Tan Y, et al. Regenerating urethral striated muscle by CRISPRi/dCas9-KRAB-mediated myostatin silencing for obesity-associated stress urinary incontinence. *CRISPR J.* 2020;3:562–572. DOI: 10.1089/crispr.2020.0077.
14. Wang L, Lin G, Lee YC, et al. Transgenic animal model for studying the mechanism of obesity-associated stress urinary incontinence. *BJU Int.* 2017;119:317–324. DOI: 10.1111/bju.13661.
15. Lee HK, Lim HM, Park SH, et al. Knockout of hepatocyte growth factor by CRISPR/Cas9 system induces apoptosis in hepatocellular carcinoma cells. *J Pers Med.* 2021;11. DOI: 10.3390/jpm11100983.
16. Lin G, Xin Z, Zhang H, et al. Identification of active and quiescent adipose vascular stromal cells. *Cytotherapy.* 2012;14:240–246. DOI: 10.3109/14653249.2011.627918.
17. Lin G, Wang G, Banie L, et al. Treatment of stress urinary incontinence with adipose tissue-derived stem cells. *Cytotherapy.* 2010;12:88–95. DOI: 10.3109/14653240903350265.
18. Lin G, Shindel AW, Banie L, et al. Molecular mechanisms related to parturition-induced stress urinary incontinence. *Eur Urol.* 2009;55:1213–1222. DOI: 10.1016/j.eururo.2008.02.027.
19. Roman W, Gomes ER. Nuclear positioning in skeletal muscle. *Semin Cell Dev Biol.* 2018;82:51–56. DOI: 10.1016/j.semcdb.2017.11.005.
20. Kass EM, Jasin M. Collaboration and competition between DNA double-strand break repair pathways. *FEBS Lett.* 2010;584:3703–3708.

21. Zhang S, Shen J, Li D, et al. Strategies in the delivery of Cas9 ribonucleoprotein for CRISPR/Cas9 genome editing. *Theranostics.* 2021;11:614–648. DOI: 10.7150/thno.47007.
22. Liang Z, Chen K, Li T, et al. Efficient DNA-free genome editing of bread wheat using CRISPR/Cas9 ribonucleoprotein complexes. *Nat Commun.* 2017;8:14261. DOI: 10.1038/ncomms14261.
23. Vakulskas CA, Dever DP, Rettig GR, et al. A high-fidelity Cas9 mutant delivered as a ribonucleoprotein complex enables efficient gene editing in human hematopoietic stem and progenitor cells. *Nat Med.* 2018;24:1216–1224. DOI: 10.1038/s41591-018-0137-0.
24. Lattanzi A, Meneghini V, Pavani G, et al. Optimization of CRISPR/Cas9 delivery to human hematopoietic stem and progenitor cells for therapeutic genomic rearrangements. *Mol Ther.* 2019;27:137–150. DOI: 10.1016/j.ymthe.2018.10.008.
25. Chandrasekaran AP, Song M, Kim KS, et al. Different methods of delivering CRISPR/Cas9 into cells. *Prog Mol Biol Transl Sci.* 2018;159:157–176. DOI: 10.1016/bs.pmbts.2018.05.001.
26. Dever DP, Bak RO, Reinisch A, et al. CRISPR/Cas9 beta-globin gene targeting in human haematopoietic stem cells. *Nature.* 2016;539:384–389. DOI: 10.1038/nature20134.
27. Shalem O, Sanjana NE, Hartenian E, et al. Genome-scale CRISPR-Cas9 knockout screening in human cells. *Science.* 2014;343:84–87. DOI: 10.1126/science.1247005.
28. Xie F, Ye L, Chang JC, et al. Seamless gene correction of β-thalassemia mutations in patient-specific iPSCs using CRISPR/Cas9 and piggyBac. *Genome Res.* 2014;24:1526–1533. DOI: 10.1101/gr.173427.114.
29. Nelson CE, Hakim CH, Ousterout DG, et al. In vivo genome editing improves muscle function in a mouse model of Duchenne muscular dystrophy. *Science.* 2016;351:403–407. DOI: 10.1126/science.aad5143.
30. Gómez-SanMiguel AB, Villanúa MÁ, Martín AI, et al. D-TRP(8)-γMSH prevents the effects of endotoxin in rat skeletal muscle cells through TNFα/NF-KB signalling pathway. *PLoS One.* 2016;11:e0155645. DOI: 10.1371/journal.pone.0155645.
31. Hurley MS, Flux C, Salter AM, et al. Effects of fatty acids on skeletal muscle cell differentiation in vitro. *Br J Nutr.* 2006;95:623–630. DOI: 10.1079/bjn20051711.
32. Lee SJ. Targeting the myostatin signaling pathway to treat muscle loss and metabolic dysfunction. *J Clin Invest.* 2021;131:e148372. DOI: 10.1172/JCI148372.
33. McPherron AC, Lawler AM, Lee SJ. Regulation of skeletal muscle mass in mice by a new TGF-beta superfamily member. *Nature.* 1997;387:83–90. DOI: 10.1038/387083a0.
34. Rao S, Fujimura T, Matsunari H, et al. Efficient modification of the myostatin gene in porcine somatic cells and generation of knockout piglets. *Mol Reprod Dev.* 2016;83:61–70. DOI: 10.1002/mrd.22591.
35. Graham ZA, De Gasperi R, Bauman WA, et al. Recombinant myostatin reduces highly expressed microRNAs in differentiating C2C12 cells. *Biochem Biophys Rep.* 2017;9:273–280. DOI: 10.1016/j.bbrep.2017.01.003.
36. Zhu X, Topouzis S, Liang L-F, et al. Myostatin signaling through Smad2, Smad3 and Smad4 is regulated by the inhibitory Smad7 by a negative feedback mechanism. *Cytokine.* 2004;26:262–272. DOI: 10.1016/j.cyto.2004.03.007.
37. Guo W, Flanagan J, Jasuja R, et al. The effects of myostatin on adipogenic differentiation of human bone marrow-derived mesenchymal stem cells are mediated through cross-communication between Smad3 and Wnt/beta-catenin signaling pathways. *J Biol Chem.* 2008;283:9136–9145. DOI: 10.1074/jbc.M708968200.
38. Tee JM, van Rooijen C, Boonen R, et al. Regulation of slow and fast muscle myofibrillogenesis by Wnt/beta-catenin and myostatin signaling. *PLoS One.* 2009;4:e5880. DOI: 10.1371/journal.pone.0005880.
39. Ge L, Dong X, Gong X, et al. Mutation in myostatin 3′UTR promotes C2C12 myoblast proliferation and differentiation by blocking the translation of MSTN. *Int J Biol Macromol.* 2020;154:634–643. DOI: 10.1016/j.ijbiomac.2020.03.043.
40. Zhang W, Wang SY, Deng SY, et al. MiR-27b promotes sheep skeletal muscle satellite cell proliferation by targeting myostatin gene. *J Genet.* 2018;97:1107–1117.
41. Liu J, Pan M, Huang D, et al. Myostatin-1 inhibits cell proliferation by inhibiting the mTOR signal pathway and MRFs, and activating the ubiquitin-proteasomal system in skeletal muscle cells of Japanese Flounder *Paralichthys olivaceus*. *Cells.* 2020;9:2376. DOI: 10.3390/cells9112376.
42. Huang Z, Chen D, Zhang K, et al. Regulation of myostatin signaling by c-Jun N-terminal kinase in C2C12 cells. *Cell Signal.* 2007;19:2286–2295. DOI: 10.1016/j.cellsig.2007.07.002.
43. Bataille S, Chauveau P, Fouque D, et al. Myostatin and muscle atrophy during chronic kidney disease. *Nephrol Dial Transplant.* 2021;36:1986–1993. DOI: 10.1093/ndt/gfaa129.
44. Yang S, Liu Y, Li MY, et al. FOXP3 promotes tumor growth and metastasis by activating Wnt/β-catenin signaling pathway and EMT in non-small cell lung cancer. *Mol Cancer.* 2017;16:124. DOI: 10.1186/s12943-017-0700-1.

Received: January 13, 2022
Accepted: March 22, 2022
Online Publication Date: June 21, 2022
Issue Publication: August 26, 2022